Nanowiring by Molecules

F. Remacle,[†,‡,§] I. Willner,[||] and R. D. Levine*[,†,||]

The Fritz Haber Research Center for Molecular Dynamics and Institute of Chemistry, The Hebrew University of Jerusalem, Jerusalem 91904, Israel, and Département de Chimie, B6c, Université de Liège, B4000 Liège, Belgium

Received: June 4, 2004; In Final Form: August 31, 2004

Microelectronic sensors require the nanowiring of a selectively active site to an electrode. Different molecules can be used as the bridge that establishes the electrical communication. We report computational results for the current carried by molecules tethered between two gold clusters as a function of the overvoltage. The computations include the effect of the voltage at the ab initio level. The trends are consistent with the currents as measured by electrochemical means and suggest that the rate of charge migration can reach far higher values than measured given somewhat higher applied bias or the application of a gate voltage. The role of polarization of the molecular charge density by the applied voltage can be quite significant with definite propensity for the orientation of the molecular charge density with respect to the field. Conduction spectroscopy is therefore analogous to optical spectroscopy in strong laser fields where the field is not a weak probe but dresses the system and can be used to control it.

1. Introduction

The rate at which electrons migrate through biological molecules generally falls exponentially with distance.[1−8] To communicate electrically to an electrode, it is therefore very beneficial to have units that can act as electron mediators.[9,10] To complete the circuit, it is necessary to connect the mediator to an electrode by a molecular linker. In this paper we discuss the electrical conduction of such linkers, which consist of a molecular bridge chemically linked to the gold atoms. We compare our computational results with electrochemical experiments that measure the current when a redo enzyme is wired to a gold electrode via a gold nanoparticle.[11] The bridge is between the gold dot and the gold electrode. We report computations for both the molecules reported in ref 11 and other molecules tested in the same way. We conclude that while chemical intuition serves well in choosing suitable bridges there can be surprises, e.g., efficient conduction by short saturated thiols. We report that, even for small voltages, because they are applied over a narrow gap, the electric transmission of the molecule depends on the field and the σ bonds are more sensitive in this respect.

The computations are in three parts and are discussed in sections 2−4, respectively. First, quantum chemical methods, with optimization of the geometry, are used to determine the electronic orbital structure of the extended molecule, that is, the dithio bridge tethered between gold atoms, in the presence of the uniform external electric field. We do so using a standard molecular approach[12−16] and the implementation of the Gaussian 03 package,[17] where the external field is applied over a finite region much larger than the molecule so that the boundary conditions remain that of an isolated molecule. This approach (further discussed in the Appendix) is different from that adopted in solid-state-based approaches where periodic boundary conditions are applied, see for example, refs 18 and 19.

Molecular orbitals (MOs) whose electron density is oriented along the direction of the uniform external electric field are more distorted (and hence conduct less well) than MOs whose electron density is perpendicular to it. Alkane bridges with σ bonds are therefore more affected by the field than conjugated bridges where typically the HOMO is of π symmetry. Also, because the electronic charge density shifts in the direction of the applied electric field, the field effects can be different for positive and negative voltages. In addition, when the conducting MOs are close in energy, as is the case for the alkanes, the field effect on the current is significant because the orbitals are mixed by the field. We emphasize that the orbitals are computed for the linker, namely, for a molecule coupled by an S atom on either end to a gold trimer. Therefore, the electrical linker as computed here includes not only the molecule but also the metal atoms it is directly bound to and the next metal atoms. This implies that the mixing of the orbitals of the molecular bridge and of the gold atoms it is bound to is implemented to all orders by the ab initio electronic computation.

The field-adapted linker orbitals are used to compute the electrical transmission of the bridge as a function of energy for a given applied voltage (section 2). The computation[20,21] is based on a scattering formalism using the generalized Ehrenfest theorem.[22] This theorem allows us to compute the quantum mechanical rate of charge migration. We obtain a Landauer-like[23] expression similar to that derived by others.[18,24−32] To bring the result to a physically transparent form, we use only the resonant part of the transmission. This is because the transmission is from a gold atom on one end of the linker to a gold atom on the other. Our final expression is therefore the current due to a coherent resonant mechanism. Because of the polarization of the orbitals by the electrical field, the transmission function and hence the current can be quite different for different applied voltages.

The voltage drop between the two electrodes (and the temperature) determines the range of energies that contribute to the conduction. The transmission function is used to compute

* To whom correspondence should be addressed. E-mail: rafi@fh.huji.ac.il. Fax: 972-2-6513742.

† The Fritz Haber Research Center for Molecular Dynamics, The Hebrew University of Jerusalem.

‡ Université de Liège.

§ Maître de Recherches, FNRS, Belgium.

|| Institute of Chemistry, The Hebrew University of Jerusalem.

10.1021/jp047591q CCC: $27.50
Published on Web 10/29/2004

the current through the molecule vs the voltage applied by integrating over all the allowed energies. When the voltage applied is comparable to the spacing between the orbitals of the bridge, we find that there can be increments in the current as additional molecular orbitals contribute to the conduction. As is known in electrochemistry[33] we find that also the current through a molecular linker increases exponentially with the overvoltage.

For a homologous series the computed current is found to decrease exponentially with the length of the molecular bridge. For example, for alkanedithiol chains we find that the scale parameter is $\beta \approx 1.1$ Å^{-1}, in agreement with other experimental[6,34−41] and theoretical[42,43] values. The value of β quoted is for the range of voltage, roughly 0.1−0.4 V, where there is no strong polarization of the charge density. As we discuss below the value of the decay parameter can depend on the strength of the externally applied voltage, in agreement with experimental results.[39,44]

Field effects can also be used to tune the conduction by shifting the position in energy of the orbitals of the bridge with respect to that of the electrodes. This can be done in two different ways. One is to use a gating configuration, where a second external field is applied in the direction perpendicular to the molecular backbone. Computing such an effect is demanding because it is a function of the strength of both fields, but the effect is there[21](see also refs 45−47), and further work is in progress in this direction. As a guide to the expected effect we discuss changing the nature of the electrodes and thereby the location of their Fermi level with respect to the energies of the electronic states of the bridge.

2. Ab Initio Electronic Structure and Geometry

We consider dithiol molecular bridges, of the generic form S−bridge−S, tethered between two gold trimers, which mimic those metallic atoms of the electrodes directly interacting with the molecular bridges. We investigated four conjugated bridges, C_6H_4, $C_6H_4-C_6H_4$, $C_6H_4-C_2-C_6H_4$, and $CH_2-C_6H_4-CH_2$, and three alkane bridges, $(CH_2)_n$, $n = 3, 6, 9$. The electronic structure computations[17] are carried out at the DFT/B3LYP[48] level with a 6-31G(d) basis set for S, C, and H and the relativistic effective core potentials of Hay and Wadt[49] (LANL2DZ) for the gold atoms. This allows us to retain a one-electron description for molecular conduction while including a part of the electron correlation. The geometry optimization includes the gold trimers and is performed at zero electric field. For all the systems investigated, it was checked that the resulting configurations are equilibrium geometries with positive vibrational frequencies. For some of the bridges, geometry optimizations have been performed with a different DFT functional (BP86) and with different basis sets for S, C, and H: 3-21G(d) and 6-31G(d,p). Except for the value of the HOMO−LUMO gap, which depends on the DFT functional, this did not lead to significant differences in the equilibrium geometries and in the MO electronic densities.

For all the different bridges, we systematically find that the isomer where a single gold atom is linked to the sulfur, $(Au)_2-Au-S-$bridge$-S-Au-(Au)_2$, is more stable by about 0.5 eV/molecule than the configuration where the S atom is bound to two Au atoms ($Au-(Au)_2-S-$bridge$-S-(Au)_2-Au$). RHF level computations using the same basis set lead to the same S−Au bonding for the most stable isomer.[15] This is in agreement with the experimental mechanism for the formation of the thio−gold bond[50] and shows that geometry optimization captures the essential feature of the Au−S bond important for conduction. In the gold trimer, all the Au atoms have the same connectivity and are equivalent for binding to the S atom. For larger sizes of the cluster where the Au atoms have different connectivity, the S−(Au_2) bonding has been found to be the most stable.[51,52] Note however that the type of binding depends both on the level of description of the electronic structure (DFT functional and size of the basis set) and on the multiplicity and charge of the whole system $(Au)_n-S-$bridge$-S-(Au)_n$. In addition, recent experimental results show that there may be fluctuation of the S−Au bonding when an alkanedithiol molecule embedded in a self-assembled monolayer is bound to a gold surface.[53]

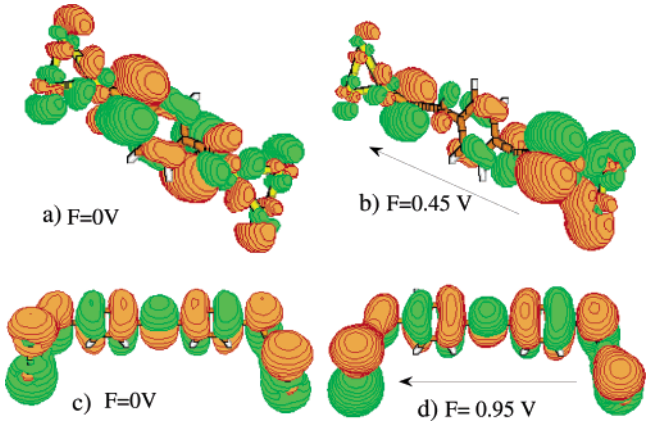

Figure 1. Charge density of the highest occupied molecular orbital, HOMO, in the absence (panels a and c) and presence (panels b and d) of a voltage applied across the molecule in the direction shown. Because the bridge is relatively short, even a low voltage corresponds to a rather high electric field. Panels a and b: $CH_2-C_6H_4-CH_2$, where the electronic density is shifted to the end of the molecule where the potential is higher. There is no significant deformation for the conjugated bridge $C_6H_4-C_2-C_6H_4$ (panels c and d).

An electric field oriented along the molecular backbone is then applied, and for each field strength the electronic structure is recomputed. The incorporation of this external electrostatic potential in a self-consistent manner is further discussed in the Appendix.

The role of the external voltage is to allow the current to flow between the two gold clusters at the two ends of the bridge. In this study, the bridge lengths vary between 0.6 and 1.3 nm. An electric field of 1 V/nm corresponds to 1.93×10^{-3} au of field. A field of 0.5 au is already sufficient to ionize a hydrogen atom in its ground state, and therefore, even low applied voltages can significantly distort the disposition of the valence electrons. For a field oriented along the molecular backbone, σ bonds will be strongly affected, with the electronic density shifting in the direction of the field, while π bonds, whose electronic density is perpendicular to the direction of the field, remain almost unaffected. We show in Figure 1 isocharge contours for the HOMO of two bridges computed at zero and at a finite field strength. For bridges where the HOMO has a σ character, such as $CH_2-C_6H_4-CH_2$ (panels a and b), the electronic density is shifted to the end of the molecule where the field strength is the strongest, while there are no significant changes for the conjugated bridge $C_6H_4-C_2-C_6H_4$ (panels c and d).

3. Transmission Function

The transmission function, $T(E)$, is computed for a resonant, through-bond, coherent transfer across the linker.[20] This means that either an electron transfers from the bulk of the electrode into an empty orbital of the linker and then to an empty orbital of the other electrode or an electron transfers from an occupied orbital of the linker to an empty orbital of the other electrode and then an electron transfers from the electrode to the hole in the previously occupied orbital of the linker. This second

mechanism can be described in a language similar to that of the first one by saying that it is a hole transfer through an occupied orbital. Which mechanism operates depends on whether an empty or an occupied orbital of the linker is within the Fermi window of energies spanned by the electrodes. Primarily, the applied voltage determines the width of this window, and when this voltage is higher, more than one orbital can fall within the window and contribute to the conduction. In the intermediate state there is an excess or defect of electrons on the linker. We have checked in detail that it is a reasonable approximation to invoke Koopman's theorem, meaning that an electron is added to an unoccupied orbital of the neutral linker or removed from an occupied orbital. In this case the transmission function takes the form of a weighted density of molecular orbitals:[20,21]

$$T(E) = \sum_{\mu} P_{\mu} \delta(E - E_{\mu}) \tag{1}$$

E_{μ} is the energy of the MO μ, and P_{μ} is given by the product of the weights of the MO μ on the atoms that are linked to the right and the left electrodes. In eq 1, we replaced the Lorentzian broadening due to the coupling to the electrode by a δ function. As we discussed elsewhere in detail,[20,21] this is justified by the fact that the width of the Fermi window due to thermal averaging is larger that the width due to the coupling to the electrodes (see eqs 3 and 4). Except at very low temperatures and voltages, systems where the molecule−electrode coupling is strong enough so that the orbital is broadened more than the Fermi width are yet to be realized. In this study, we take P_{μ} to be given by the weights of the MO μ on the Au atoms bound to the sulfurs on the left, Au_l, and on the right, Au_r, leading to

$$P_{\mu} = \sum_{i=1}^{N_{AO}} |c_{i\mu}^{Au_l}|^2 |c_{i\mu}^{Au_r}|^2 \tag{2}$$

N_{AO} is the number of atomic orbitals used to describe the Au atoms in the ab initio computation. The important point is that P_{μ} is given by the product of the weights of the MO on the left and right ends of the molecule. For the resonance transmission of a given MO μ, $T(E_{\mu})$, to be large, the MO needs to have significant weight on both ends. If the direction of the field is such that, for a given MO, the electronic density is shifted to one end of the molecule, this particular MO will conduct less. On the other hand, the opposite direction of the field will favor conduction by making the weight more evenly distributed over both ends. This effect is present for most of the MOs of the alkane bridges because they are of σ character. Such an effect is shown in Figure 2 for the hexanedithio bridge, where $T(E)$ is plotted as a function of energy for zero field (panel a) and the two possible directions of a field oriented along the molecular backbone (panels b and c).

Unlike the saturated alkanes, in most conjugated bridges the highest occupied MOs are of π symmetry and hence are more protected from the effect of a field between the two electrodes. This is shown graphically in Figure 3 for the transmission function of $S-C_6H_4-C_2-C_6H_4-S$. This means that conjugated bridges will continue to conduct when the field strength is increased further. As can be seen by comparing Figures 2 and 3, for the conjugated bridges, the HOMO lies higher in energy and the HOMO−LUMO gap is smaller than for the alkane bridges. This explains why unsaturated bridges are better conductors. The HOMO can be accessed for lower values of the applied bias than in the case of the alkane bridges. In the systems investigate here, conduction occurs via holes since it is the HOMO that is the closest in energy to the gold Fermi level. It takes much stronger applied bias to see the contribution of electron conduction to the current.

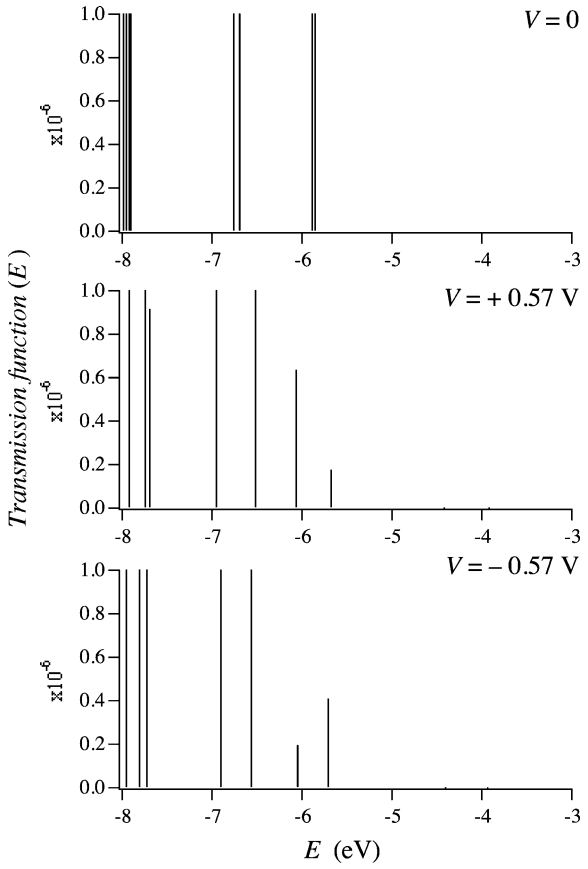

Figure 2. Transmission function (eq 1) as a function of energy (eV) for the $Au_2-Au-S-(CH_2)_6-S-Au-Au_2$ bridge. Panel a: The ab initio computation (for details see section 2) is for a zero field along the molecular backbone. The HOMO and HOMO − 1 are almost degenerate. Each of them is localized at one of the two $Au-S-CH_2$ ends of the hexane bridge. In panel b the external field is applied along the molecular backbone in the positive direction. The field mixes the two highest occupied MOs shown in panel a, and their energy difference increases. The result is a decrease of the intensity of $T(E)$, the HOMO being less conducting than the HOMO − 1. In panel c, the external field is applied in the opposite direction. The split of the MOs is the same, but now the HOMO is more conducting than the HOMO − 1, so that, at low values of the applied bias, the current is higher for negative than for positive fields.

A second effect of the external field arises when there are MOs that are nearly degenerate. If these MOs are coupled by the field, they will repel, and the effect of the field is to induce additional nonlinearities in the $I-V$ curves. Since the density of the MO is rather sparse, it is however less important in the present study than in our work on arrays of quantum dots.[21]

4. Current vs Applied Bias

Current vs applied bias curves are plotted in Figure 4. To convert the applied bias to an overpotential requires knowing the value of the redox potential of the reference electrode used in electrochemical studies. The Fermi energy, E_{Fermi}, of the gold electrode is equal to −5.53 eV and close to the energy of the HOMO of the bridges investigated here. The higher orbital, the LUMO, is typically at ∼−4.2 eV. Conduction occurs therefore via "hole migration". To observe conduction by electron migration, one would need to use electrodes with different Fermi energy or to move the energy levels of the bridge by applying a gating voltage.[21,45−47] We compute the current using a scattering theory formalism[22] similar to the Landauer ap-

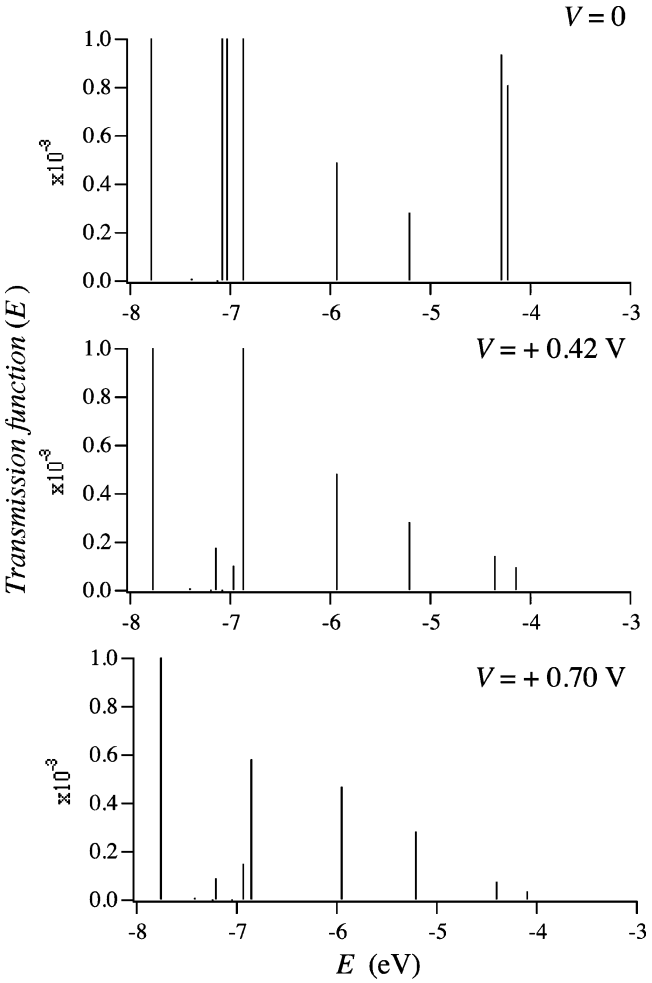

Figure 3. Transmission function as a function of energy computed for $Au_2-Au-S-C_6H_4-C_2-C_6H_4-S-Au-Au_2$ at zero field (panel a), 0.42 V (panel b), and 0.70 V (panel c) along the molecular backbone. The HOMO falls at −5.2 eV and is of π character (see Figure 1). Its electronic density and its energy are almost not affected by the external field. On the other hand, the LUMO and LUMO + 1 orbitals have a more pronounced σ character and are localized each at one end of the bridge. They are almost degenerate and effectively coupled by the field.

proach.[18,23−32,54,55] It is given by averaging the transmission function over the one-electron states of the electrodes:[20]

$$I = \frac{2\pi e}{h}\sum_{\mu} g(\epsilon_\mu,V,T)\; T_V(E_\mu) \qquad (3)$$

$g(\epsilon_\mu,V,T)$ is the Fermi window[21]

$$g(\epsilon_\mu,V,T) = f_{\text{left}}(E_\mu - E_{\text{Fermi}} - eV/2) - f_{\text{right}}(E_\mu - E_{\text{Fermi}} + eV/2) \quad (4)$$

that is centered about the Fermi energy, E_{Fermi}, and has a width that equals the applied voltage V with rounded wings due to the finite temperature T. The onset of conduction is a rising exponential function of the applied voltage and occurs when the wings of the Fermi window begin to overlap with the HOMO. The inset in Figure 4 shows the same curves computed in the approximation where the effect of the voltage is not included in the computation of the MOs. Note how propane, whose bonds are only of σ type, becomes a less good conductor when the field is included in the computation of the transmission function. Other bridges affected by the field but to a lesser extent are methylphenyl, where the HOMO has a partial σ character

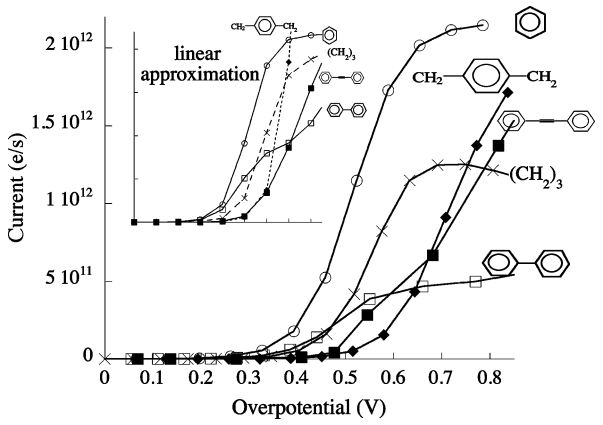

Figure 4. Current (number of electrons transmitted per second, e/s) vs applied bias (V) for a number of thiol bridges, as identified in the figure, between gold trimers. The inset (same axes and same symbols as the main plot) is a simpler computation where the same transmission function is used for all values of the applied bias. It is labeled "linear" because for very weak voltages this approximation leads to Ohm's law. The primary effect of including the distortion of the molecular charge density by the applied voltage is to significantly reduce the conduction of σ-bonded molecules. Possibly this is the real reason alkanes are reputedly not good conductors because in the linear regime, see the inset, they conduct quite well.

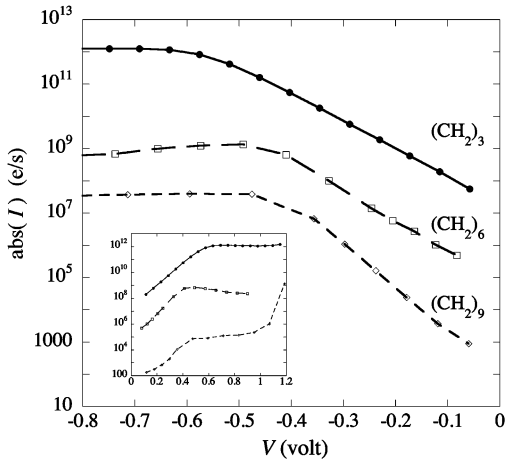

Figure 5. Absolute value of the current (e/s on a log scale) vs negative applied bias (V) for dithiopropane, -hexane, and -nonane bridges. These curves are used to determine the value of the decay constant β (see Figure 6). For positive values of the applied bias (shown in the inset), the $I-V$ curves are less monotone, and the value of the current is smaller. This is due to the fact that, for positive values of the applied bias (see Figure 2), the $T(E)$ of the HOMO is smaller than the $T(E)$ of the HOMO − 1. A positive applied bias disfavors conduction, while a negative applied bias assists conduction.

on the methyl ends (see Figure 1a,b), and biphenyl. In the biphenyl bridge, at equilibrium, the angle between the two phenyls is 34°, so that a field applied in the direction of the σ-skeleton of one of the phenyls will have a component in the direction perpendicular to the second phenyl group and distort the charge density. The $I-V$ curves of phenyl and diphenylethylene bridges are almost identical in the linear approximation and when the field effect is included in the computation of the electronic structure.

5. Scaling of the Conductivity with Distance

Within a homologous series the computed rate of transport is found to decrease exponentially with the bridge length. For example, Figure 5 shows $I-V$ curves for dithiopropane, -hexane, and -nonane tethered between two gold trimers. The effect of

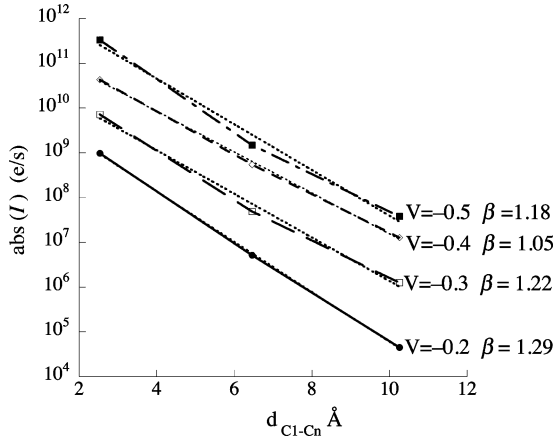

Figure 6. Absolute value of the current (e/s on a log scale) vs the C_1-C_n distance for the dithiopropane, -hexane, and -nonane bridges, shown for four values of the applied bias. The fits to $A + \exp(-\beta d_{C_1-C_n})$ are shown as dotted lines. β is expressed in inverse angstroms. The obtained value depends on the strength of the applied bias, but for voltages below 1 V the range is in agreement with experimental and simpler models; see the text.

the field is included on the electronic structure computation. The figure shows the current computed for negative voltages, while the inset is for positive bias. From Figure 5, one can see that the value of β, the distance scaling constant of the rate of charge migration, depends on the voltage. We show in Figure 6 the value of the current for a given voltage as a function of the C−C distance between the two ends of the chain (Å). We choose the negative bias portion of the $I-V$ curves because the current varies more monotonically with the voltage than the positive range (inset of Figure 5). One can see from Figure 6 that the fitted values for β vary between 1.29 $Å^{-1}$ for $V = -0.2$ V and 1.05 $Å^{-1}$ for $V = -0.4$ V. The decrease of β with increasing voltage is consistent with the experimental results reported in ref 39. These values, obtained from ab initio computation including field effects, are in agreement with both the experimental[6,34−38] values measured in solution and the computed[39,42,43] ones using simpler models for describing the electronic structure. We note that the way the length of the chain is estimated also matters. What was used here is the projection of the C_1-C_n distance on the field direction. When β is computed per methylene unit, values between 1.35 and 1.66 $Å^{-1}$ per methylene are obtained, in good agreement with the factor 1.25 $Å^{-1}$ per methylene used in the literature.[38,56]

A simple exponential decline of the rate with distance requires that the molecular "wire" is chemically homogeneous. Already some time ago[57] we saw that it is possible to slow the rate significantly by introducing electron-attracting groups along the bridge.

6. Effect of the Position of the Fermi Level

The current as shown above is computed for a Fermi energy of gold of −5.53 eV. Conductivity is maximal when the Fermi energy matches the orbital energy of the linker, and for many molecular bridges this means that for gold electrodes conduction is by holes migrating through the HOMO. By using different electrodes, we can change this picture, and the common electrochemical practice of using two different electrodes may be the simplest route for exploring the mechanism of conduction by molecules. The effect of varying the Fermi energies is shown in Figure 7 for the benzene and dimethylbenzene bridges. While for the gold Fermi energy benzene is a much better conductor than dimethylbenzene, dimethylbenzene becomes progressively a better conductor for $E_{\text{Fermi}} < 5.55$ eV. Another way to control

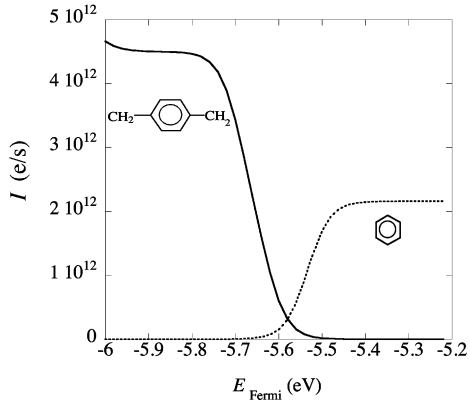

Figure 7. Current (e/s) as a function of the Fermi level of the electrodes (eV) for the benzene and the dimethylbenzene bridges, computed for an applied bias of 0.5 V.

the current is to apply a voltage in a direction perpendicular to the molecule. Our computations[21] and others[45−47] suggest that such a "gate" voltage can be used to significantly alter the current.

7. Concluding Remarks

We compared the computed conductivities of different conjugated and nonconjugated organic spacers linked on both sides to small gold clusters with electrochemical results. The computation of the current uses a scattering approach and is based on an ab initio determination of the geometry and molecular levels of the gold−spacer−gold system at the DFT and RHF levels. The effects of the external electric field are investigated at the DFT level. At low values of the applied bias, short saturated spacers are found to be as good conductors as conjugated molecules. The conductivity drops exponentially with the length of the spacer, but longer nonconjugated spacers can be better conductors at higher values of the applied bias or/and if a gating voltage is applied. The role of the electric field in determining the current means that conductivity is not a spectroscopic probe of the electronic structure of the unperturbed molecule. Rather, it provides much richer information because it shows how the structure of the molecule deforms in response to the field.

Acknowledgment. We thank H. B. Gray and E. S. Kryachko for useful comments on different aspects of the problem. This work is supported by the US-Israel Binational Science Foundation, Jerusalem, Israel. The computational work used facilities provided by NIC (University of Liège) and SFB 377 (The Hebrew University of Jerusalem). The work of F.R. is supported by Grant RW.115012 (Région Wallonne) and ARC (University of Liège). F.R. is a Maître de Recherches, FNRS, Belgium.

Appendix

The effect of the voltage is incorporated into the computation by representing it as an external dipolar field.[58] This field is included as part of the Hamiltonian in the quantum chemistry code using boundary conditions for an isolated molecule and a localized basis set. For an overall neutral molecule submitted to an external uniform electric field, **E**, the energy of interaction of the charges (nuclei and electrons) of the system with the external field is a dipolar term. This amounts to adding a term—$\boldsymbol{E}\cdot\boldsymbol{r}$—in the Kohn−Sham equations that are solved self-consistently:

$$\left(-\frac{1}{2}\nabla^2 + V_{\text{H}}(\mathbf{r}) + V_{\text{ex}} - \mathbf{E}\cdot\mathbf{r}\right)\tilde{\phi}_i = \tilde{\epsilon}_i\tilde{\phi}_i$$

where $\tilde{\phi}_i$ and $\tilde{\epsilon}_i$ are the uniform external electric field self-consistent molecular orbitals and the corresponding energies. $V_H(\mathbf{r})$ is the Hartree potential. It is the local potential due to the electrostatic Coulomb interactions. V_{ex} is the exchange potential and is nonlocal. The molecular orbitals $\tilde{\phi}_i$ define the electronic density $\tilde{\rho}(\mathbf{r})$, which by definition is related to the Hartree potential by

$$V_H(\mathbf{r}) = \int d\mathbf{r}' \frac{\tilde{\rho}(\mathbf{r}')}{|\mathbf{r} - \mathbf{r}'|} - \sum_{\alpha=1}^{N} \frac{Z_\alpha}{|\mathbf{r} - \mathbf{R}_\alpha|}$$

where the index α refers to the nuclei. The Hartree potential in the presence of an external uniform electric field inherently satifies the Poisson equation:

$$\nabla^2 V_H(\mathbf{r}) = -4\pi\tilde{\rho}(\mathbf{r}) - \sum_\alpha Z_\alpha \delta(\mathbf{r}-\mathbf{R}_\alpha) = -4\pi\rho_{Tot}(\mathbf{r})$$

$V_H(\mathbf{r})$ is also referred to in quantum chemistry as the molecular electrostatic potential.[59] The difference between $V_H(\mathbf{r})$ in the presence and in the absence of the electric field is often used to get a better understanding of how the potential drops along the molecular backbone.[14,19,60,61] We will discuss elsewhere the features of the electrostatic potential for the molecular bridges reported here.

References and Notes

(1) Winkler, J. R.; Gray, H. B. *Chem. Rev.* **1992**, *92*, 369.
(2) McLendon, G. *Acc. Chem. Res.* **1988**, *21*, 160.
(3) Bixon, M.; Giese, B.; Wessely, S.; Langenbacher, T.; Michel-Beyerle, M. E.; Jortner, J. *Proc. Natl. Acad. Sci. U.S.A.* **1999**, *96*, 11713.
(4) Wan, C. Z.; Fiebig, T.; Schiemann, O.; Barton, J. K.; Zewail, A. H. *Proc. Natl. Acad. Sci. U.S.A.* **2000**, *97*, 14052.
(5) Carell, T.; Behrens, C.; Gierlich, J. *Org. Biomol. Chem.* **2003**, *1*, 2221.
(6) Smalley, J. F.; Finklea, H. O.; Chidsey, C. E. D.; Linford, M. R.; Creager, S. E.; Ferraris, J. P.; Chalfant, K.; Zawodzinsk, T.; Feldberg, S. W.; Newton, M. D. *J. Am. Chem. Soc.* **2003**, *125*, 2004.
(7) Gray, H. B.; Winkler, J. R. *Q. Rev. Biophys.* **2003**, *36*, 341.
(8) Adams, D. M.; Brus, L.; Chidsey, C. E. D.; Creager, S.; Creutz, C.; Kagan, C. R.; Kamat, P. V.; Lieberman, M.; Lindsay, S.; Marcus, R. A.; Metzger, R. M.; Michel-Beyerle, M. E.; Miller, J. R.; Newton, M. D.; Rolison, D. R.; Sankey, O.; Schanze, K. S.; Yardley, J.; Zhu, X. Y. *J. Phys. Chem. B* **2003**, *107*, 6668.
(9) Willner, I.; Heleg-Shabtai, V.; Blonder, R.; Katz, E.; Tao, G.; Bückmann, A. F.; Heller, A. *J. Am. Chem. Soc.* **1996**, *118*, 10321.
(10) Hess, C. R.; Juda, G. A.; Dooley, D. M.; Amii, R. N.; Hill, M. G.; Winkler, J. R.; Gray, H. B. *J. Am. Chem. Soc.* **2003**, *125*, 7156.
(11) Xiao, Y.; Patolsky, F.; Katz, E.; Hainfeld, J. F.; Willner, I. *Science* **2003**, *299*, 1877.
(12) Karzari, Y.; Cornil, J.; Bredas, J. L. *J. Am. Chem. Soc* **2001**, *123*, 10076.
(13) Derosa, P. A.; Seminario, J. M. *J. Phys. Chem. B* **2001**, *105*, 471.
(14) Weber, H. B.; Reichert, J.; Weigend, F.; Ochs, R.; Beckmann, D.; Mayor, M.; Ahlrichs, R.; Lhoneysen, H. v. *Chem. Phys.* **2002**, *281*, 113.
(15) Remacle, F.; Levine, R. D. *Chem. Phys. Lett.* **2004**, *383*, 537.
(16) Basch, H.; Ratner, M. A. *J. Chem. Phys.* **2004**, *120*, 5761.
(17) Frisch, M. J.; Trucks, G. W.; Schlegel, H. B.; Scuseria, G. E.; Robb, M. A.; Cheeseman, J. R.; Montgomery, J. A., Jr.; Vreven, T.; Kudin, K. N.; Burant, J. C.; Millam, J. M.; Iyengar, S. S.; Tomasi, J.; Barone, V.; Mennucci, B.; Cossi, M.; Scalmani, G.; Rega, N.; Petersson, G. A.; Nakatsuji, H.; Hada, M.; Ehara, M.; Toyota, K.; Fukuda, R.; Hasegawa, J.; Ishida, M.; Nakajima, T.; Honda, Y.; Kitao, O.; Nakai, H.; Klene, M.; Li, X.; Knox, J. E.; Hratchian, H. P.; Cross, J. B.; Adamo, C.; Jaramillo, J.; Gomperts, R.; Stratmann, R. E.; Yazyev, O.; Austin, A. J.; Cammi, R.; Pomelli, C.; Ochterski, J. W.; Ayala, P. Y.; Morokuma, K.; Voth, G. A.; Salvador, P.; Dannenberg, J. J.; Zakrzewski, V. G.; Dapprich, S.; Daniels, A. D.; Strain, M. C.; Farkas, O.; Malick, D. K.; Rabuck, A. D.; Raghavachari, K.; Foresman, J. B.; Ortiz, J. V.; Cui, Q.; Baboul, A. G.; Clifford, S.; Cioslowski, J.; Stefanov, B. B.; Liu, G.; Liashenko, A.; Piskorz, P.; Komaromi, I.; Martin, R. L.; Fox, D. J.; Keith, T.; Al-Laham, M. A.; Peng, C. Y.; Nanayakkara, A.; Challacombe, M.; Gill, P. M. W.; Johnson, B.; Chen, W.; Wong, M. W.; Gonzalez, C.; Pople, J. A. *Gaussian 03*, revision B.04; Gaussian, Inc.: Pittsburgh, PA, 2003.
(18) Datta, S. *Electronic Transport in Mesoscopic Systems*; Cambridge University Press: Cambridge, U.K., 1995.
(19) Liang, G. C.; Ghosh, A. W.; Paulsson, M.; Datta, S. *Phys. Rev. B* **2004**, *69*, 115302.
(20) Remacle, F.; Levine, R. D. *Isr. J. Chem.* **2003**, *42*, 269.
(21) Remacle, F.; Beverly, K. C.; Heath, J. R.; Levine, R. D. *J. Phys. Chem. B* **2003**, *107*, 13892.
(22) Levine, R. D. *Quantum Mechanics of Molecular Rate Processes*; Dover: New York, 1999.
(23) Landauer, R. *IBM J. Res. Dev.* **1957**, *1*, 223.
(24) Lang, N. D. *Phys. Rev. B* **1995**, *52*, 5335.
(25) DiVentra, M.; Pantelides, S. T.; Lang, N. D. *Phys. Rev. Lett.* **2000**, *84*, 979.
(26) Mujica, V.; Kemp, M.; Ratner, M. A. *J. Chem. Phys* **1994**, *101*, 6849.
(27) Emberly, E. G.; Kirczenow, G. *Phys. Rev. B* **1998**, *58*, 10911.
(28) Hall, L. E.; Reimers, J. R.; Hush, N. S.; Silverbrook, K. *J. Chem. Phys.* **2000**, *112*, 1511.
(29) Nitzan, A. *Annu. Rev. Phys. Chem.* **2001**, *52*, 681.
(30) Xue, Y. Q.; Datta, S.; Ratner, M. A. *Chem. Phys.* **2002**, *281*, 151.
(31) Taylor, J.; Brandbyge, M.; Stokbro, K. *Phys. Rev. Lett.* **2002**, *89*, 138301.
(32) Gutierrez, R.; Grossmann, F.; Schmidt, R. *ChemPhysChem* **2003**, *4*, 1252.
(33) Ulstrup, J. *Charge Transfer Processes in Condensed Media*; Springer-Verlag: Berlin, 1979.
(34) Chidsey, C. E. D. *Science* **1991**, *251*, 919.
(35) Smalley, J. F.; Feldberg, S. W.; Chidsey, C. E. D.; Linford, M. R.; Newton, M. D.; Liu, Y. P. *J. Phys. Chem.* **1995**, *99*, 13141.
(36) Terrill, R. H.; Postlethwaite, T. A.; Chen, C. H.; Poon, C. D.; Terzis, A.; Chen, A. D.; Hutchison, J. E.; Clark, M. R.; Wignall, G.; Londono, J. D.; Superfine, R.; Falvo, M.; Johnson, C. S.; Samulski, E. T.; Murray, R. W. *J. Am. Chem. Soc.* **1995**, *117*, 12537.
(37) Sachs, S. B.; Dudek, S. P.; Hsung, R. P.; Sita, L. R.; Smalley, J. F.; Newton, M. D.; Feldberg, S. W.; Chidsey, C. E. D. *J. Am. Chem. Soc* **1997**, *119*, 10563.
(38) Wuelfing, W. P.; Green, S. J.; Pietron, J. J.; Cliffel, D. E.; Murray, R. W. *J. Am. Chem. Soc.* **2000**, *122*, 11465.
(39) Cui, X. D.; Primak, A.; Zarate, X.; Tomfohr, J.; Sankey, O. F.; Moore, A. L.; Moore, T. A.; Gust, D.; Nagahara, L. A.; Lindsay, S. M. *J. Phys. Chem. B* **2002**, *106*, 8609.
(40) Xu, B.; Tao, N. J. *Science* **2003**, *301*, 1221.
(41) Salomon, A.; Cahen, D.; Lindsay, S.; Tomfohr, J.; Engelkes, V. B.; Frisbie, C. D. *Adv. Mater.* **2003**, *15*, 1881.
(42) Newton, M. D. *Chem. Rev.* **1991**, *91*, 767.
(43) Hsu, C. P.; Marcus, R. A. *J. Chem. Phys.* **1997**, *106*, 584.
(44) Wang, W. Y.; Lee, T.; Reed, M. A. *Phys. Rev. B* **2003**, *68*, 035416.
(45) Rashkeev, S. N.; DiVentra, M.; Pantelides, S. T. *Phys. Rev. B* **2002**, *66*, 033301.
(46) DiVentra, M.; Pantelides, S. T.; Lang, N. D. *Appl. Phys. Lett.* **2000**, *76*, 3448.
(47) Ghosh, A. W.; Rakshit, T.; Datta, S. *Nano Lett.* **2004**, *4*, 565.
(48) Becke, A. D. *J. Chem. Phys.* **1993**, *98*, 5648.
(49) Hay, P. J.; Wadt, W. R. *J. Chem. Phys.* **1985**, *82*, 299.
(50) Finklea, H. A. Au-S bond formation mechanism. In *Electroanalytical Chemistry*; Bard, A. J., Rubinstein, I., Eds.; Marcel Dekker: New York, 1996; Vol. 19, p 109.
(51) Basch, H.; Ratner, M. A. *J. Chem. Phys.* **2003**, *119*, 11926.
(52) Remacle, F.; Kryachko, E. S. *J. Mol. Struct.*, in press.
(53) Ramachandran, G. K.; Hopson, T. J.; Rawlett, A. M.; Nagahara, L. A.; Primak, A.; Lindsay, S. M. *Science* **2003**, *300*, 1413.
(54) Imry, Y. *Introduction to Mesoscopic Physics*; Oxford University Press: Oxford, U.K., 2002.
(55) Nitzan, A.; Ratner, M. A. *Science* **2003**, *300*, 1384.
(56) Hicks, J. F.; Templeton, A. C.; Chen, S.; Sheran, K. M.; Jasti, R.; Murray, R. W. *Anal. Chem.* **1999**, *71*, 3703.
(57) Remacle, F.; Levine, R. D.; Ratner, M. A. *Chem. Phys. Lett.* **1998**, *285*, 25.
(58) Cohen-Tannoudji, C.; Diu, B.; Laloe, F. *Quantum Mechanics*; Wiley: New York, 1977.
(59) Johnson, B. G.; Gill, P. M.; Pople, J. A. *Chem. Phys. Lett.* **1993**, *206*, 239.
(60) Mujica, V.; Roitberg, A. E.; Ratner, M. *J. Chem. Phys* **2000**, *112*, 6834.
(61) Xue, Y. Q.; Ratner, M. A. *Phys. Rev. B* **2003**, *68*, 115406.